

Subharmonic resonance of global climate to solar forcing

A. Bershadskii

ICAR, P.O.B. 31155, Jerusalem 91000, Israel

It is shown that, the wavelet regression detrended fluctuations of the monthly global temperature data (land and ocean combined) for the period 1880-2009yy, are completely dominated by one-third subharmonic resonance to annual forcing (both natural and anthropogenically induced). Role of the oceanic Rossby waves and the resonance contribution to the *El Niño* phenomenon have been discussed in detail.

PACS numbers: 92.70.Gt, 92.70.Qr, 92.10.am, 92.10.Hm

INTRODUCTION

The monthly global temperature data are known to be strongly fluctuating. Actually, the fluctuations are of the same order as the trend itself (see figures 1 and 2). While the nature of the trend is widely discussed (in relation to the global warming) the nature of these strong fluctuations is still quite obscure. The problem has also a technical aspect: detrending is a difficult task for such strong fluctuations. In order to solve this problem a wavelet regression detrending method was used in present investigation. Then a spectral analysis of the detrended data reveals rather surprising nature of the strong global temperature fluctuations. Namely, the detrended fluctuations of the global temperature for the last century (the instrumental monthly data are available at Ref. [1], see also Ref. [2]) are completely dominated by so-called one-third subharmonic resonance to annual forcing.

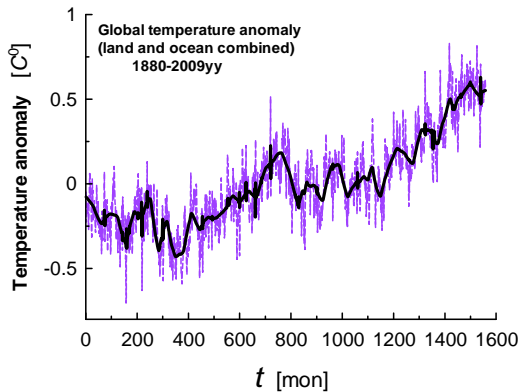


FIG. 1: The monthly global temperature data (dashed line) for the period 1880-2009. The solid curve (trend) corresponds to a wavelet (symmlet) regression of the data.

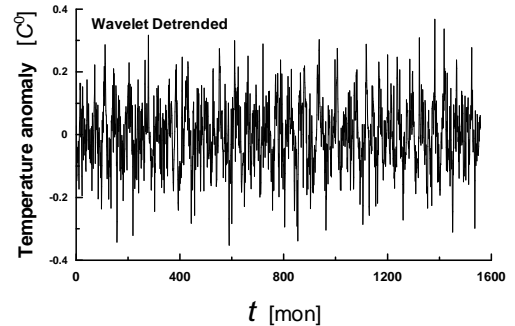


FIG. 2: The wavelet regression detrended fluctuations from the data shown in Fig. 1.

SUBHARMONIC RESONANCE TO ANNUAL FORCING

There are many well known reasons for asymmetry in response of the North and South Hemispheres to solar forcing: dominance of water in the Southern Hemisphere against dominance of land in the Northern one, topographical imbalance of land (continents) and oceans in the Northern Hemisphere due to continental configuration, seasonality and vegetation changes are much more pronounce on land than on ocean surface, and anthropogenically induced asymmetry of the last century. This asymmetry results in *annual* asymmetry of global heat budget and, in particular, in annual fluctuations of the global temperature. Nonlinear responses are expected as a result of this asymmetry.

Figure 1 shows (as dashed line) the instrumental monthly global temperature data (land and ocean combined) for the period 1880-2009, as presented at the NOAA site [1]. The solid curve (trend) in the figure corresponds to a wavelet (symmlet) regression of the data (cf Refs. [3],[4]). Figure 2 shows corresponding detrended fluctuations, which produce a statistically stationary set of data. Most of the regression methods are linear in responses. At the nonlinear nonparametric wavelet regression one chooses a relatively small number of wavelet

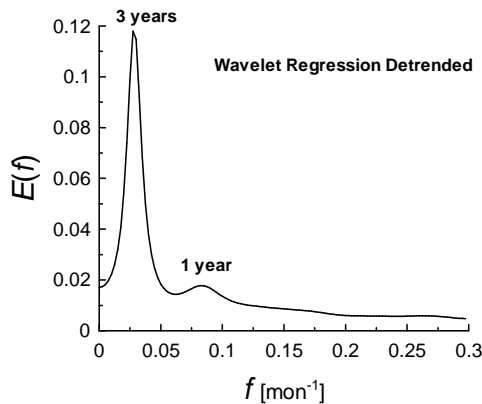


FIG. 3: Spectrum of the wavelet regression detrended fluctuations of the monthly global temperature anomaly (land and ocean combined).

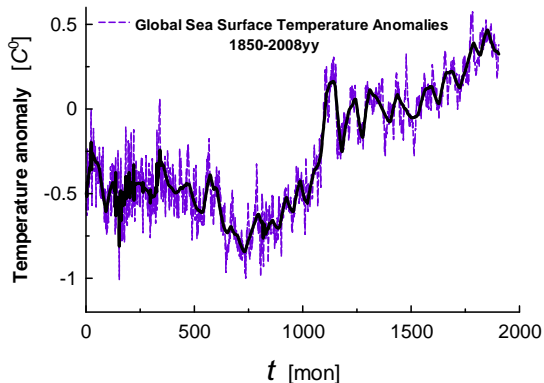


FIG. 4: The monthly global Sea Surface Temperature Anomalies (dashed line) for the period 1850-2008yy (the data taken from Ref.[17]). The solid curve (trend) corresponds to a wavelet (symmlet) regression of the data.

coefficients to represent the underlying regression function. A threshold method is used to keep or kill the wavelet coefficients. In this case, in particular, the Universal (VisuShrink) thresholding rule with a soft thresholding function was used. At the wavelet regression the demands to smoothness of the function being estimated are relaxed considerably in comparison to the traditional methods. Figure 3 shows a spectrum of the wavelet regression detrended data calculated using the maximum entropy method (because it provides an optimal spectral resolution even for small data sets). One can see in this figure a small peak corresponding to a one-year period and a huge well defined peak corresponding to a three-

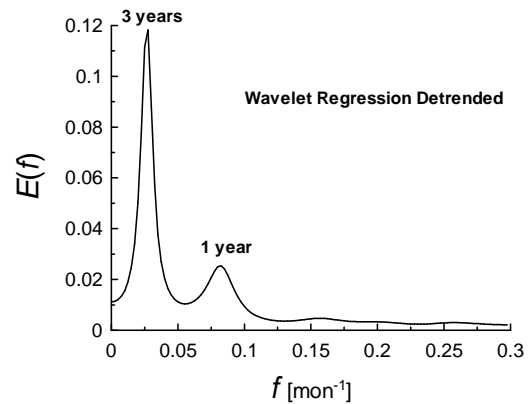


FIG. 5: The same as in Fig. 3 but for the wavelet regression detrended fluctuations of the global Sea Surface Temperature Anomalies.

years period.

In order to understand underlying physics of the very characteristic picture shown in the Fig. 3 let us imagine a forced excitable system with a large amount of loosely coupled degrees of freedom schematically represented by Duffing oscillators (which has become a classic model for analysis of nonlinear phenomena and can exhibit both deterministic and chaotic behavior [5]-[8] depending on the parameters range) with a wide range of the natural frequencies ω_0 (it is well known [9] that oscillations with a wide range of frequencies are supported by ocean and atmosphere, cf also Ref. [10]):

$$\ddot{x} + \omega_0^2 x + \gamma \dot{x} + \beta x^3 = F \sin \omega t \quad (1)$$

where \dot{x} denotes the temporal derivative of x , β is the strength of nonlinearity, and F and ω are characteristic of a driving force. It is known (see for instance Ref. [11]) that when $\omega \approx 3\omega_0$ and $\beta \ll 1$ the equation (1) has a resonant solution

$$x(t) \approx a \cos\left(\frac{\omega}{3}t + \varphi\right) + \frac{F}{(\omega^2 - \omega_0^2)} \cos \omega t \quad (2)$$

where the amplitude a and the phase φ are certain constants. This is so-called one-third subharmonic resonance with the driving frequency ω corresponding to the *annual* NS-asymmetry of the solar forcing (the huge peak in Fig. 3 corresponds to the first term in the right-hand side of the Eq. (2)). For the considered system of the oscillators an effect of synchronization can take place and, as a consequence of this synchronization, the characteristic peaks in the spectra of partial oscillations coincide [12]. It can be useful to note, for the global climate modeling, that the odd-term subharmonic resonance is a consequence of

ROLE OF ROSSBY WAVES

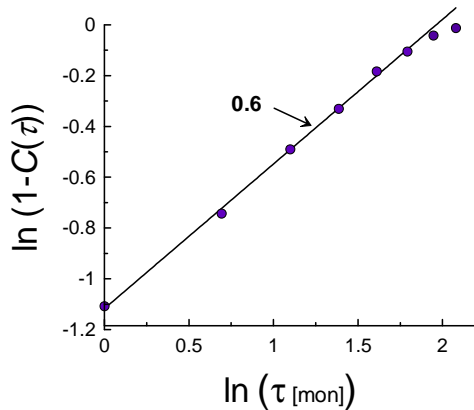


FIG. 6: Defect of autocorrelation function versus τ (in ln-ln scales) for the wavelet regression detrended fluctuations of the global Sea Surface Temperature Anomalies. The straight line is drawn in order to indicate scaling Eq. (3).

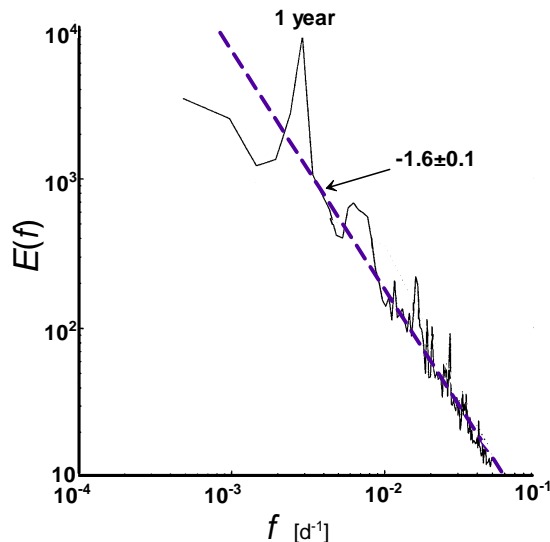


FIG. 7: Spectrum of sea surface height fluctuations [15] (TOPEX/ Poseidon and ERS-1/2 altimeter measurements) in the logarithmic scales. The profound peak corresponds to the annual cycle. The dashed straight line is drawn in order to indicate correspondence to the scaling Eq. (3).

the reflection symmetry of the natural nonlinear oscillators (invariance to the transformation $x \rightarrow -x$, cf. also Ref. [13]).

The fluctuations of oceanic temperature cause certain variations of the sea surface height. These variations are intermixed with the sea surface height variations caused by the oceanic planetary Rossby waves. The oceanic planetary Rossby waves play an important role in the response of the global ocean to the forcing (see, for instance, Refs. [14],[15]) and they are of fundamental importance to ocean circulation on a wide range of time scales (it was also suggested that the Rossby waves play a crucial role in the initiation and termination of the *El Niño* phenomenon, see also below). Therefore, they present a favorable physical background for the global subharmonic resonance. For that reason it is interesting to look also separately at global sea surface temperature anomalies. These data for time range 1850-2008yy are shown in Fig. 4 (the monthly data were taken from Ref. [17], see also Ref. [18]). The solid curve (trend) in the figure corresponds to the wavelet (symmlet) regression of the data. Figure 5 shows a spectrum of the wavelet regression detrended data calculated using the maximum entropy method. The spectrum seems to be very similar to the spectrum presented in Fig. 3.

Since the high frequency part of the spectrum is corrupted by strong fluctuations (the Nyquist frequency equals $0.5 [mon^{-1}]$), it is interesting to look at corresponding autocorrelation function $C(\tau)$ in order to understand what happens on the monthly scales. It should be noted that scaling of defect of the autocorrelation function can be related to scaling of corresponding spectrum:

$$1 - C(\tau) \sim \tau^\alpha \quad \Leftrightarrow \quad E(f) \sim f^{-(1+\alpha)} \quad (3)$$

Figure 6 shows the defect of the autocorrelation function in ln-ln scales in order to estimate the scaling exponent $\alpha \simeq 0.6 \pm 0.04$ (the straight line in this figure indicates the scaling Eq. (3)). The existence of oceanic Rossby waves was confirmed rather recently by NASA/CNES TOPEX/Poseidon satellite altimetry measurements. Corresponding to these measurements spectrum of the sea surface height fluctuations, calculated in Ref. [15] with *daily* resolution (see also [16]), is shown in Figure 7. The dashed straight line in this figure is drawn in order to indicate correspondence to the scaling Eq. (3): $1 + \alpha \simeq 1.6$.

EL NINO PHENOMENON

The Rossby waves (together with Kelvin waves) and a strong atmosphere-ocean feedback provide physical background for the *El Niño* phenomenon (see, for instance, Ref. [19] and references therein). Figure 9 shows spectrum for the wavelet detrended fluctuations

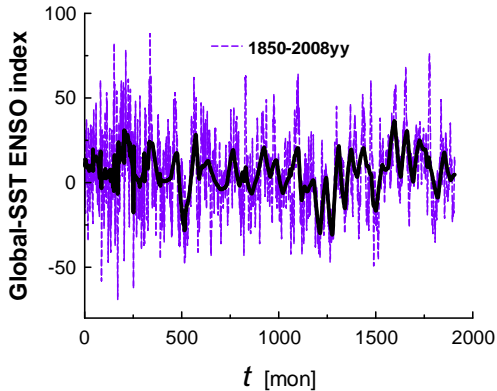


FIG. 8: The monthly Global-SST ENSO index (dashed line) for the period 1850-2008yy (the data taken from Ref. [20], the index is in hundredths of a degree Celsius) . The solid curve (trend) corresponds to a wavelet (symmlet) regression of the data.

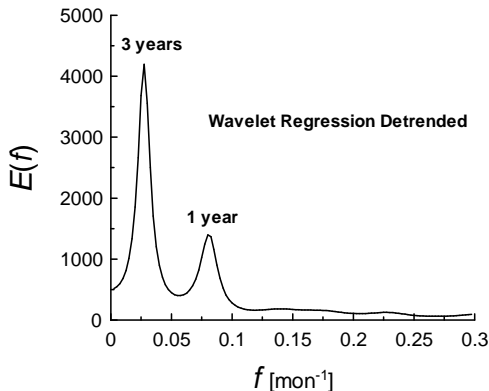


FIG. 9: The same as in Fig. 3 but for the wavelet regression detrended fluctuations of the Global-SST ENSO index.

of the so-called Global-SST ENSO index (Fig. 8), which captures the low-frequency part of the *El Niño* phenomenon (the monthly data are available at Ref. [20]). The annual forcing can come from the oceanic Rossby waves (cf Fig. 7). To support this relationship we show in figure 10 defect of autocorrelation function calculated using the wavelet detrended fluctuations from Fig. 8. The \ln - \ln scales have been used in Fig. 10 in order to estimate the scaling exponent $\alpha \simeq 0.6 \pm 0.03$ (the straight line in this figure indicates the scaling Eq. (3), cf Figs. 6 and 7). Using these observations one can suggest that the *El Niño* phenomenon has the one-third subharmonic resonance as a background.

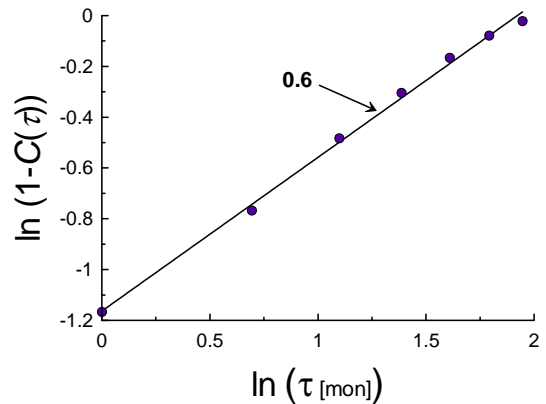


FIG. 10: The same as in Fig. 6 but for the wavelet regression detrended fluctuations of the Global-SST ENSO index.

The data were provided by National Climatic Data Center at NOAA and by Joint Institute for the Study of the Atmosphere and Ocean. I also acknowledge that a software provided by K. Yoshioka was used at the computations.

-
- [1] The data are available at <http://lwf.ncdc.noaa.gov/oa/climate/research/anomalies/index.html>
 - [2] T.M. Smith, et al., Improvements to NOAA's Historical Merged Land-Ocean Surface Temperature Analysis (1880-2006), *J. Climate*, **21**, 2283 (2008).
 - [3] N. Scafetta, and B. J. West, Phenomenological solar contribution to the 1900-2000 global surface warming, *Geophys. Res. Lett.*, **33**, L05708 (2006).
 - [4] T. Ogden, *Essential Wavelets for Statistical Applications and Data Analysis* (Birkhauser, Basel, 1997).
 - [5] E. Ott, *Chaos in Dynamical Systems* (Cambridge University Press, 2002).
 - [6] D. Permann and I. Hamilton, Wavelet analysis of time series for the Duffing oscillator: The detection of order within chaos, *Phys. Rev. Lett.*, **69**, 2607 (1992).
 - [7] V. Brunnsden and P. Holmes, Power spectra of strange attractors near homoclinic orbits, *Phys. Rev. Lett.*, **58**, 1699 (1987).
 - [8] A. Bershadskii, Chaotic climate response to long-term solar forcing variability, *EPL (Europhys. Lett.)*, **88**, 60004 (2009).
 - [9] S.M. Tobias, and N.O. Weiss, Resonant Interactions between Solar Activity and Climate, *J. Climate*, **13**, 3745 (2000).
 - [10] J. Brindley, T. Kapitaniak, and A. Barcion, Chaos and noisy periodicity in forced ocean-atmosphere models, *Phys. Lett. A*, **167**, 179-184 (1992).
 - [11] A.H. Nayfeh and D.T. Mook, "Nonlinear Oscillations" (John Wiley & Sons, a Wiley-Interscience Publication, 1979).

- [12] Yu.I. Neimark and P.S. Landa, *Stochastic and Chaotic Oscillations*, (Dordrecht, Kluwer, 1992).
- [13] S. Minobe, and F-f Jin., Generation of interannual and interdecadal climate oscillations through nonlinear sub-harmonic resonance in delayed oscillators, *Geophys. Res. Lett.*, **31**, L16206, (2004).
- [14] P.S. Polito, and W.T. Liu, Global characterization of Rossby waves at several spectral bands, *J. Geophys. Res. - Oceans*, **108**, 3018 (2003).
- [15] X. Zang and C. Wunsch, Spectral description of low frequency oceanic variability, *J. Phys. Oceanogr.*, **31** 3073 (2001).
- [16] X. Zang, L.L. Fu, and C. Wunsch, Observed reflectivity of the western boundary of the equatorial Pacific Ocean. *J. Geophys. Res.*, **107**, 3150 (2002).
- [17] The data are available at http://jisao.washington.edu/data/global_sstanomts/
- [18] T.M. Smith, et al., Reconstruction of historical sea surface temperatures using empirical orthogonal functions, *J. Climate*, **9**, 1403 (1996).
- [19] E. Tziperman, H. Scher, S.E. Zebiak and M. A. Cane, Controlling Spatiotemporal Chaos in a Realistic El Nino Prediction Model, *Phys. Rev. Lett.*, **79**, 1034-37 (1997).
- [20] The data are available at <http://jisao.washington.edu/data/globalstenso/>